

# Efforts to Reduce Part Bed Thermal Gradients during Laser Sintering Processing

Mengqi Yuan\* and David Bourell\*

\*Laboratory for Freeform Fabrication, Mechanical Engineering Department  
The University of Texas at Austin, TX 78712  
REVIEWED, Accepted August 15, 2012

## Abstract

Part bed surface thermal gradients (x-y plane) are usually present in laser sintering (LS) fabricators. The purpose of this study was to investigate various means to reduce these thermal gradients. Several experiments were conducted using a FLIR™ infrared camera to examine the thermal profile of the part bed during the LS operation. Experiments included thermal profile characterization of the part bed with different nitrogen shielding gas flow rates, assessment of the proper experimental settings, and a temperature profile record of the part bed from the warm-up to the cool-down stage. A series of experiments were conducted using the laser as a heat source to preheat part bed surface cold spots to decrease the thermal gradients, which effect was limited by the natural low thermal conductivity of nylon 12 powder and large heat convection. Moreover, manifolds were mounted below the piston to provide warm nitrogen down draft flow during the LS operation.

## Introduction

Laser sintering is an additive manufacturing technology that uses a high power laser to fuse polymer powder into a mass that has a desired three-dimensional shape. The laser selectively scans and fuses powder material on the surface of the powder bed based on a previously generated CAD file. After one layer is scanned, the powder bed is lowered by one layer thickness, creating a new layer that is scanned. The process is repeated until the part is completed [1]. This process has the potential to be a valuable industrial tool [2]. Thermal processing during the LS operation is essential in improving the efficiency of the process and the accuracy of product quality and dimension.

Polyamide 12, also known as Nylon 12, is a thermoplastic material that is widely used in laser sintering. It has high elongation, good abrasion resistance, good specific strength, and melts at a temperature around 180°C [1]. Thermal management and heat transfer analysis of polyamide 12 in the LS part bed are essential to better understand the effect of processing on the service part properties and performance.

Temperature distribution of powder bed during LS has been analyzed in different materials including metal, polymer, etc. Some were focused on the surface temperature distribution, while some others were about the LS operation chamber. S. Kolossov *et.al* [3] developed a 3D thermal model of LS using finite element simulation, which incorporated the nonlinear behavior of the titanium powder. They found the temperature profiles during LS operation along both X- and Y-axes reached a maximum around 2500°C in the middle of the axes, and decreased to 500- 750°C on both sides. These results were in agreement with the infrared red camera experiments.

Moreover, the only temperature profile examined was during the stable heat-up period; it is unknown how the part bed temperature profile behaved during LS processing which is an important part of the overall thermal exposure.

There is a relation that illustrates the laser energy density with the laser power and beam properties:

$$\rho = \frac{P}{DV} \quad (1)$$

where  $\rho$  is laser energy density (LaserED), P is laser power, D is laser beam diameter, and V is the scan speed [3].

S. Kumpaty, D. Cottrill *et al.* [4] analyzed the heat transfer process in the Sinterstation<sup>®</sup> 2500Plus during the part build, recording the changes in Duraform<sup>®</sup> polyamide powder temperature using an infrared thermocouple. First, with the part bed at 149°C, tests were conducted on three square discs with 7,9,11 Watts of laser power. It was found the part bed temperature increased with increasing laser power. Second, the temperature profile of a single layer was explored. A valley was created on the temperature profile when cooler powder was spread over the part bed (140-150 °C). Temperature increased in the sintering process (170-175 °C), and then the part bed powder cooled and solidified and the temperature stabilized around 161°C until the roller deposited a fresh layer of powder over the top surface. Last, a relation between the laser power and the temperature rise was found:

$$T = 1.6111 + 0.6761P \quad (2)$$

where T is the temperature rise from 6 to 9 °C, P is the laser power from 6 to 12 Watts. Eq. (2) shows the temperature rise is proportional to the power increment, which is constant with Eq. (1), which shows the laser energy density is proportional to the power. However, the value of this prediction is limited due to the limited power range, and the thermocouple was found accumulated with powder at the end of the experiment. In addition, the sensor measurement circle is relatively small comparing to the part bed, which led to the experiment inaccuracy.

Franco, M. Lanzetta and L. Romoli [5] conducted experiments to assess the energetic aspects of LS using polyamide 12 powder, and they analyzed the energetic productivity and laser parameters. A SYNARD CO<sub>2</sub> laser was used in 3D LS machine. The energy density was varied modulating the scan speed and the laser power in the range 500-2500 mm/s and 12.5-50 W, respectively. The laser spot diameter was kept constant at 0.7 mm. A combination of 16 different groups of parameters was tested, resulting an energy density between 0.0071- 0.2857 J/mm<sup>2</sup>. Moreover, the sintered parts with different energy densities were attached at the surface of a container, which had a vibrating device beneath to measure the energetic intensity (EI). EI was found to be low ranging from 0.2- 0.6 J/mm<sup>3</sup> with respect to an ED ranging from 0.015- 0.3 J/mm<sup>2</sup>. In addition, it was found that the best results could be obtained operating with energy density between 0.02-0.08 J/mm<sup>2</sup>. Specially, the process with 0.06-0.08 J/mm<sup>2</sup> laser ED could lead to elimination of preheating phase during the LS process, since most energy (35%) was consumed by the chamber heaters.

In this research effort, a 2D thermal profile investigation on the polyamide 12 powder bed during LS operation was conducted. The effect of shielding gas flow rate and laser pre-scan treatment were investigated as means to reduce thermal gradients on the surface of the part bed during LS processing.

## **Experimental Procedure**

### **1. SS 2500 parameters**

It is important to acquire proper operating temperature on left/right feed bins and the part bed. There are basically two steps before the LS: heating to initial warm-up set-points (no powder is spread during this time); heating to operation set-points (0.1mm powder layer is spread over the surface, 25.4mm in total).

To evaluate the most proper operating temperature for the feed bins, after reaching the initial warm-up set points on feed bins (around 70 °C), feed bins set-points were manually increased by 1- 2°C after every 2-3 layers of powder were added. The maximum feed temperatures were reached when the feed bed started to show subtle cracking, or ripples were observed on the part bed surface. The proper feed heater set-points were 1 °C below the maximum feed temperature. Moreover, the set-points might be different on left and right feed bins, due to the individual heater performance and heat leakage on each side.

To evaluate the proper operating temperature for the part bed surface, careful observation of the heat fence part building is essential. First, the part bed temperature was set to a relatively low operating temperature, ~171°C). If slight curling was seen during a part build, the part bed set-point was increased by 2°C. The process was repeated until non-curling flat layers were obtained.

### **2. Thermal profile investigation**

**Apparatus** Measurements of the temperature at the surface of the part bed were made by means of an infrared (IR) camera, which was a FLIR model A325, serial 48000675 thermal imaging camera, with a 320×240 pixel resolution, 16-bit resolution, and focal length 18 mm. . The sensor in the camera measured long-wave (8-12 μm) IR radiation. For the measurement, the camera temperature range was 0-500 °C, yielding a thermal resolution of 0.03 °C. Absolute accuracy of the camera was 2 °C for known emissivity. Object emissivity was 0.825 by comparing the camera-reported temperature of a heated black body source with and without the SS 2500 front window. . Image acquisition rate was adjustable from 0-60 Hz.

The insulated viewing window in front of the SS2500 was replaced with an insulated aluminum-fiberglass panel with visible and IR transparent zinc-selenide (ZnSe) viewports. The IR camera was mounted at the front of the machine and looked through the viewports. The ZnSe window had an anti-reflective coating for a transmissivity greater than 0.98 [6]. The camera was enclosed in a fan-cooled box to protect from dust and powder. The camera was controlled by FLIR ExaminIR software. Figure 1 shows a representative thermograph from the IR camera of a heated chamber, with the nonlinear temperature scale in °C.

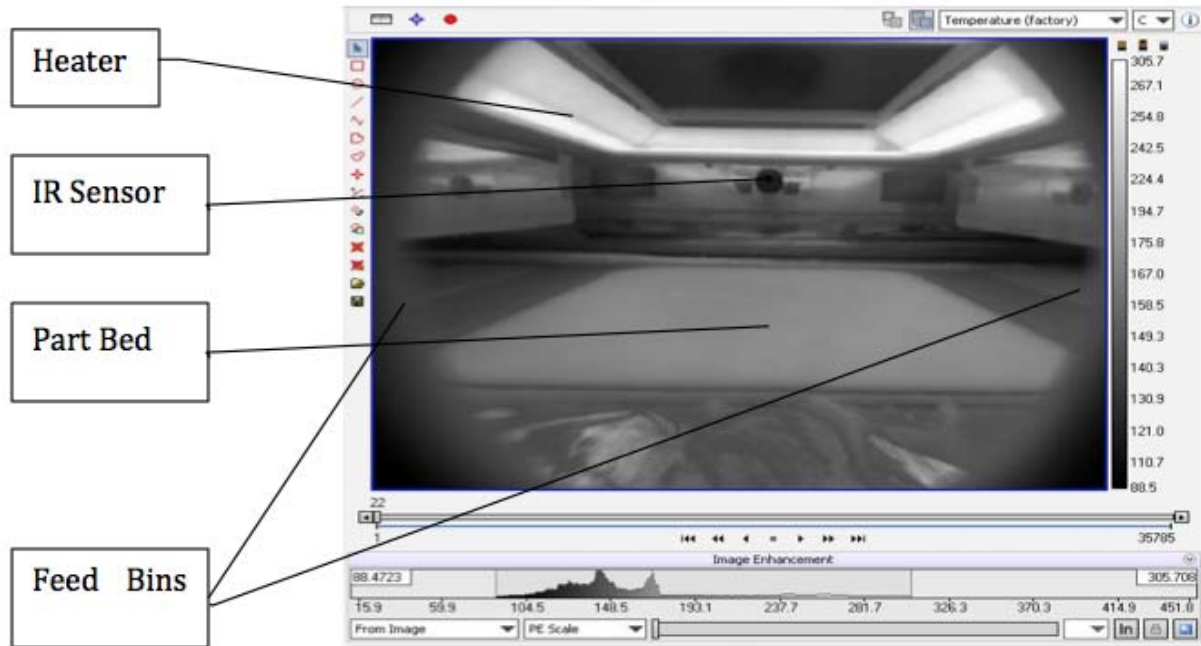


Figure 1: Build chamber in the SinterStation 2500 surface that including heater, IR sensor, part bed and two feed bins, and IR thermograph during warm-up stage.

**Procedure** To obtain a temperature profile of the part bed from heat-up to cool-down, which would last for several hours depending on the product size, the IR camera mounted on the ZnSe window was set with a data acquisition frequency of 0.5Hz. Data at every stage were recorded and exported to an Excel file and processed by MATLAB. For the warm-up stage, the part bed temperature increased after a new layer of powder was spread, and the maximum value was selected in each layer to perform a smooth plot of the part bed mean temperature. For the LS stage, the transient equilibrium temperature of the sintered part after sintering was selected and plotted to show the smooth mean temperature profile on sintered parts at different positions of the part bed. For the cool-down stage, the transient equilibrium temperature after each layer was selected and plotted.

To analyze the circulating nitrogen thermal effect on the part bed surface temperature, the part bed was heated to 175 °C. First the nitrogen flow rate was changed from 0.5 m<sup>3</sup>/h to 2.5 m<sup>3</sup>/h, increased by 0.5 m<sup>3</sup>/h incrementally and held for 5 minutes. A line in the middle of the part bed along the X- axis was observed by the IR camera to obtain a thermal profile. After that, the circulating nitrogen valve was closed and the line was observed by the IR camera for 1 hour. Thermal profiles were plotted along the X- axis at different time periods (0 second after nitrogen valve closed, 800 seconds later, 2400 seconds later, and 3600 seconds later).

### 3. Laser pre-scan treatment

One approach to achieving a more uniform part bed surface temperature is to pre-scan cooler areas with the laser spot. Referring to Eq. (1), the parameters affecting the laser energy density are the laser beam diameter, laser scan speed and laser power. The laser beam diameter is difficult to change “on the fly”, and the change of scan speed is limited with SinterStation functions. The laser scan power is easier to change and was selected as the assessment parameter.

Tests were conducted on 15 cubes ( $0.0254\text{m} \times 0.0254\text{m} \times 0.0254\text{m}$ ) with laser power varying from 0.5-7 watts. The part bed temperature was held constant at  $173\text{ }^{\circ}\text{C}$ . The space between each square along the x- and y-axes was  $0.00635\text{m}$ . The IR camera was mounted during the LS stage to acquire the temperature rise after the sintering scan with data acquisition frequency  $2\text{ Hz}$  and default emissivity  $0.825$ . The temporal duration of the temperature rise was also recorded. Graphs presenting the temperature change versus power were plotted and analyzed.

Moreover, to evaluate different powers and position effects on the products, mechanical properties of sintered tensile bars were tested using an INSTRON<sup>®</sup> Series 3340 Model 3345 Single Column Testing System, with a maximum capacity of  $5\text{kN}$  and maximum vertical test space of  $1123\text{ mm}$  [7]. Experimental data were analyzed using INSTRON Bluehill Lite software. The extension rate was set at  $2\text{ mm/min}$  with a sensitivity of  $40\%$ .

## **Results and Discussion**

### **1. SS 2500 parameters**

The SinterStation left and right feed bin and part bed operation temperatures varies by machine and heater. For the machine and heater used in this case, the left feed bin operation temperature was  $100\text{ }^{\circ}\text{C}$ , while the temperature for the right feed bin was  $93\text{ }^{\circ}\text{C}$ .

Part bed operation temperature was set at  $173\text{-}175^{\circ}\text{C}$  after several observations and experiments. Previously using a lower set point led to curling on the sintered part. Too high a setpoint melted or glazed the powder surface.

### **2. Thermal profile investigation**

Temperature changes at every stage (warm-up, LS and cool-down) were recorded by the IR camera and processed by MATLAB. Figures 2a and 2b show the actual and maximum temperature profile versus time during the warm-up stage.

Figure 2a shows that the temperature dropped  $10\text{-}20\text{ }^{\circ}\text{C}$  each time the roller spread over the polymer surface and then increased by  $1\text{-}2\text{ }^{\circ}\text{C}$  compared to last cycle maximum temperature. The maximum temperature plateaued at  $175\text{-}178\text{ }^{\circ}\text{C}$ . Figure 2b simplified the warm-up process by disregarding the inverse powder-spreading spike. The temperature increased steadily from  $148\text{ }^{\circ}\text{C}$  to  $172\text{ }^{\circ}\text{C}$  in about  $1000$  seconds then slowly reached an equilibrium around  $178\text{ }^{\circ}\text{C}$  which held for  $2700$  seconds. The equilibrium temperature starting at  $2000$  seconds was quite close to the polyamide 12 melting point of about  $180\text{ }^{\circ}\text{C}$  [1].

An IR image of LS on the powder bed surface is shown in Fig. 3. There was a  $10\text{-}15\text{ }^{\circ}\text{C}$  temperature difference on the powder bed surface between the hottest spot and coldest spot. The heater is shown all white because its temperature falls outside the measurement range. The part bed surface is hot in the middle and right corner, but cold around four sides and the upper-left corner. Convection from the environment may contribute to the thermal gradient.

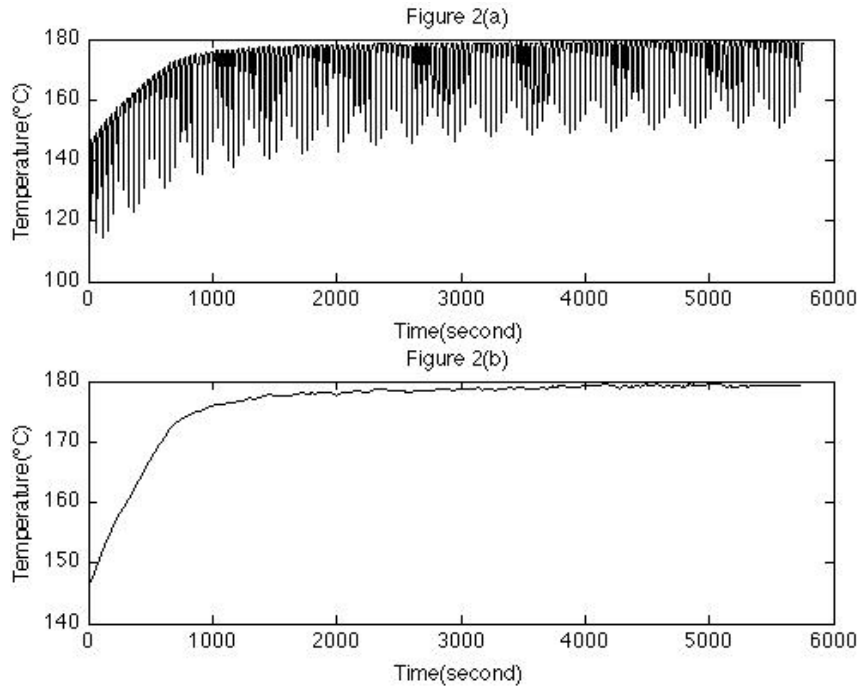


Figure 2: Polyamide 12 part bed surface temperature profile versus time in warm-up stage before LS. (a) Part bed surface mean temperature plotted by IR camera and (b) Maximum mean temperature as processed by MATLAB.

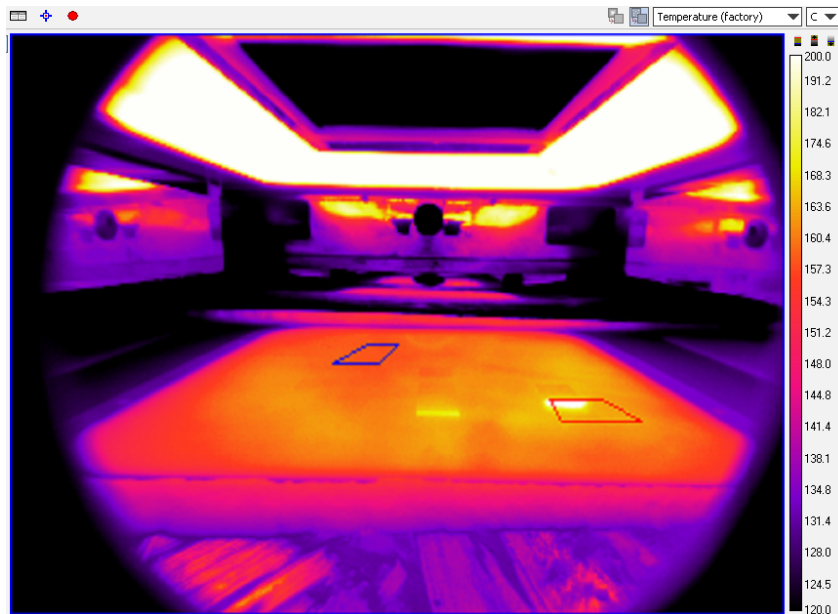


Figure 3: Thermograph from the IR camera during laser sintering. Default emissivity is set as 0.825. The temperature range was manually set to be 120- 200 °C. Two squares drawn on the surface (lower right and upper left) show a hot spot and cold spot of powder bed. The bright yellow rectangle in the middle of the part bed surface is a square that just finished being laser sintered. The brighter white rectangular spot on right was being laser sintered when the image was captured.

Figure 4a-c show powder bed surface temperature profiles during laser sintering that were recorded, exported by FLIR camera and processed by MATLAB.

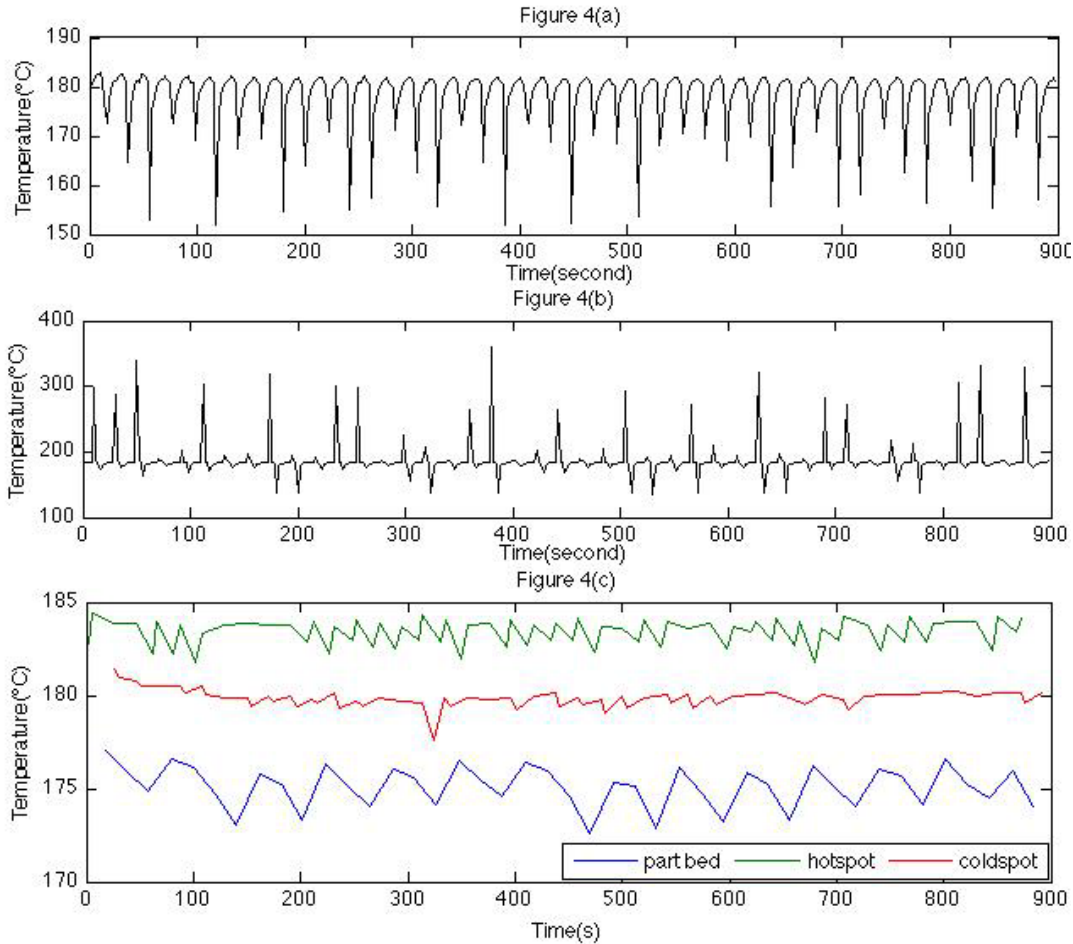


Figure 4: Polyamide 12 part bed surface temperature profile versus time during laser sintering. (a) The mean temperature of part bed surface during LS; (b) The mean temperature profile of hot spot surface during LS; (c) The mean temperature profile processed by MATLAB that includes the mean surface temperature profiles versus time for the part bed, hot spot and cold spot.

Figure 4a shows a thermal recording from the IR camera versus time for the part bed surface mean temperature during LS. A large temperature gap occurred after each 70-80 seconds indicating the moment the roller spread the powder over the surface, while the mean temperature dropped to 152-153 °C.

Figure 4b is the real-time IR record showing the hot spot mean temperature on the part bed surface versus time. The high temperatures shown (300-400 °C) were not reasonable since the part was in a melt or half-melt status, and the emissivity was changed, rendering the measurement to be inaccurate. However, it still seen that the LS process temperature was decreased by the roller spreading powder over the surface and was increased by LS.

Figure 4c shows the mean temperature profile versus time processed by MATLAB of the whole part bed, hot spot, and cold spot during the whole LS process. Each data point was selected at the moment after LS when the temperature reached equilibrium. However, the temperature data for the hot spot and cold spot were higher than 180 °C because the part was still in a “half melt” status with the emissivity changed from 0.825. In addition, the system error was included (2 °C) [6]. It is seen that the hot spot temperature was 3-5 °C higher than that of the cold spot. The part bed mean temperature was lower than both spots at around 175°C, which is quite close to the set point.

In terms of the cool-down, Figure 5a and 5b show plots of powder bed surface mean temperature change versus time via IR camera and processed by MATLAB.

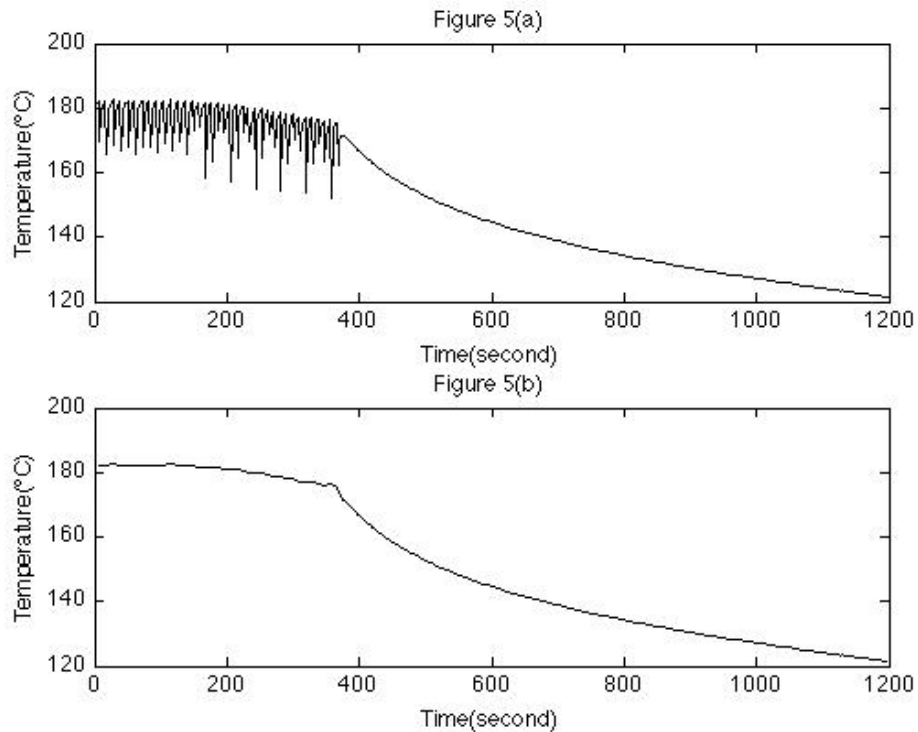


Figure 5: Polyamide 12 part bed surface temperature profile versus time during cool-down. (a) The mean temperature of part bed surface; (b) The part bed surface mean temperature profile processed by MATLAB.

Figure 5a shows that the part bed surface temperature slowly decreased 5-10 °C in 350-380 seconds and then continually decreased to 120 °C in 800 seconds. Temperature at the moment that roller spread powder over the surface decreased by 15-30 °C. Figure 5b shows a smooth plot of the part bed surface temperature.

To analyze nitrogen effects on the part bed profile, two experiments were conducted with the nitrogen purge gas on and purge gas off, respectively, which results are shown below in Figure 6.

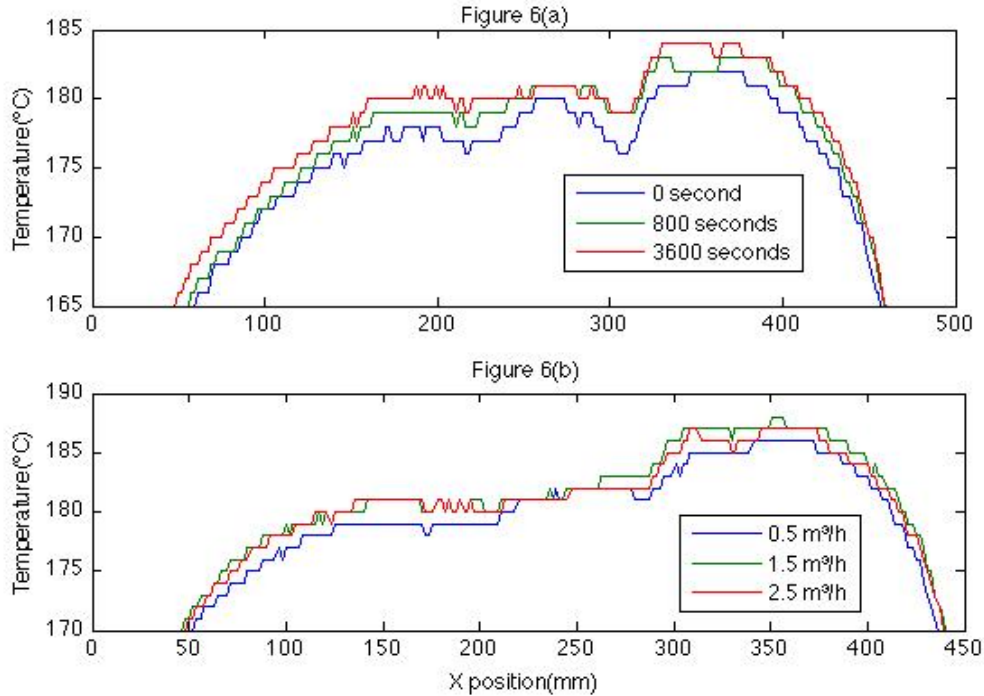


Figure 6: Nitrogen circulation effect on part bed surface temperature. (a) The mean temperature of a part bed surface middle-line along the x-axis with purge nitrogen off at the moment nitrogen was off and 800 and 3600 seconds later; (b) The mean temperature of part bed surface middle line along the x-axis with purge nitrogen on, at nitrogen rates of 0.5, 1.5, 2.5 m<sup>3</sup>/h.

Figure 6a shows that the part bed mean surface temperature increased with time after turning the circulation nitrogen off. The temperature range was selected from 165- 185 °C for better observation. The whole part bed mean temperature increased 2-3 °C after turning nitrogen off for 800 seconds and increased another 2-3 °C after 3600 seconds.

Figure 6b shows the effect of different nitrogen circulation rates on the whole part bed mean surface temperature. The temperature increased 1-2 °C after changing the nitrogen rate from 0.5 m<sup>3</sup>/h to 1.5 m<sup>3</sup>/h, and remained when the nitrogen rate was changed from 1.5 m<sup>3</sup>/h to 2.5 m<sup>3</sup>/h. Data were selected 5 mins after changing the nitrogen rate. Within the first 5 minutes, nitrogen was continuously purging and heated by the heater. So the heated nitrogen had an effect on the part bed by increasing part bed mean surface temperature. However, the part bed mean surface temperature increased when the nitrogen rate stayed in a small range. After changing the flow rate to 2.5 m<sup>3</sup>/h, the part bed temperature was the same as the part bed temperature when the flow rate was 1.5 m<sup>3</sup>/h.

### 3. Laser pre-scan treatment

The laser pre-scan experiment was conducted by building cubes on the part bed that were laser sintered by different powers ranging from 0.5 W- 7 W. The IR camera mounted on the SinterStation front window was used to record the temperature change. A thermograph during LS is shown in Figure 7.

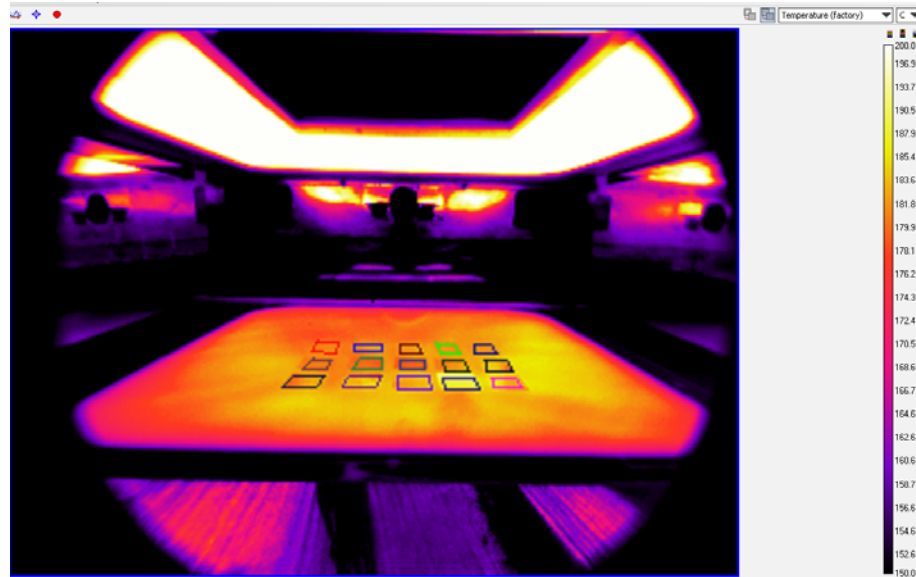


Figure 7: thermograph from IR camera during LS. The array of 15 squares denotes LS build areas, each scanned at a different laser power setting from 0.5-7 watts.

Cubes sintered by different power were highlighted by a different color, and each was separated by 0.25 inch in both x- and y-axes. Part bed operating temperature was 173 °C. The detailed temperature rise and duration are shown in Figure 8.

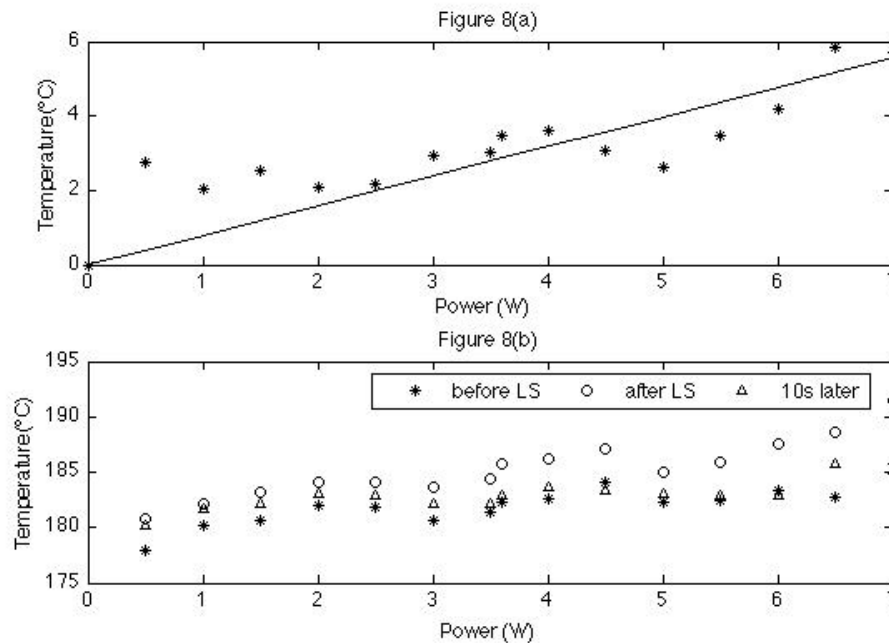


Figure 8: Temperature change of the sintered cubes by laser pre-scanning the powder bed surface. (a) Temperature rise as a function of LS power; (b) Pre-scanned part surface temperature as a function of power: before LS, after LS, and 10 seconds later after LS.

It is shown in Fig. 8a that the temperature rises roughly linearly and increases with power. Each datum was the temperature difference between the cube temperature before LS and the cube temperature immediately after LS. A linear relationship was empirically obtained for the temperature increase  $\Delta T$ :

$$\Delta T = 0.7958P \quad (3)$$

where  $\Delta T$  is the temperature difference from 0 to 6 °C, P is the laser power from 0 to 7 watts. The average residual is 0.53 in this case. It is reasonable since according to Eq. (1), laser density energy increased linearly with power change, and temperature increment presents the laser density energy increment.

Figure 8b shows the transient effect of the pre-scanned surface temperature change. It is seen that for each cube, the temperature increased 2-4 °C based on different laser powers. However, 10 seconds later, the pre-scanned surface temperature decreased back to the temperature before the scan, which means the effect dissipated quickly. This could be due to the low thermal conductivity of PA 12 (0.09-0.12 W/mK) [1] and convection.

Figure 9 shows a thermograph of sintered tensile bars in the hot spot (right side) and cold spot (upper left side) during LS.

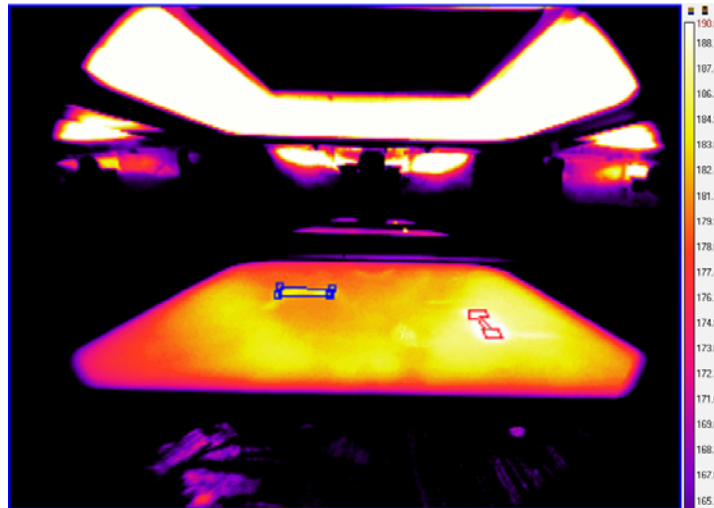


Figure 9: Thermograph of sintered tensile bars in the powder bed hot spot and cold spot. The temperature range was 165-190 °C.

First, two tensile bars were sintered with 4 watts laser power in the hot spot and cold spot; after that, two more were sintered at the same position but with 10 watts laser power. Tensile stress and elongation was assessed using an INSTRON 3340 single column testing system. The original tensile bar gauge was 17 mm. Results are shown in Table 1.

At the same position, the tensile bar sintered with larger power shows greater tensile stress. Moreover, tensile bars in the hot spot had larger tensile stress than that in the cold spot when the laser power was the same. The same situation happened in the case of elongation. These data demonstrate the importance of the powder bed surface temperature to achieve acceptable mechanical properties.

	<b>Tensile Stress (MPa)</b>	<b>Elongation (%)</b>
<b>Hotspot_4W</b>	<b>39.3</b>	<b>21.7</b>
<b>Coldspot_4W</b>	<b>20.4</b>	<b>6.5</b>
<b>Hotspot_10W</b>	<b>54.3</b>	<b>27.6</b>
<b>Coldspot_10W</b>	<b>41.6</b>	<b>24.7</b>

Table 1: Mechanical properties of tensile bars sintered at the powder bed hot spot and cold spot with different laser power.

### **Summary and Conclusion**

Various experiments were conducted to investigate and reduce thermal gradients on the part bed during LS. First, proper temperature set points for feed bins and part bed are important for LS operation. Second, thermal profile investigation provides the actual and MATLAB processed temperature profiles during the warm-up, LS, and cool-down stages. Hot spot temperature was 3-5 °C higher than that of the cold spot in LS. Third, the part bed mean surface temperature increases with time after turning the circulation nitrogen off; it increased 1-2 °C after changing the nitrogen rate from 0.5 m<sup>3</sup>/h to 1.5 m<sup>3</sup>/h, and remained when the nitrogen rate was changed from 1.5 m<sup>3</sup>/h to 2.5 m<sup>3</sup>/h. Fourth, the laser pre-scan treatment shows the sintered part temperature increases linearly with increasing laser power, but the effect dissipates quickly after 10 seconds. Last, mechanical properties were tested on tensile bars that were sintered in the hot spot and cold spot with different power, which demonstrates the importance of the powder bed surface temperature to achieve acceptable mechanical properties.

### **Acknowledgments**

The authors would like to acknowledge funding from the Air Force Research Laboratory under Grant #GRT00015778.

### **References**

- 
- [1] M. Yuan, T. Diller, D. Bourell, 2011, ‘Thermal Conductivity Measurements of Polyamide 12’, *Solid Freeform Fabrication Symposium Proceedings (427-37)*, Austin, TX.
- [2]: J. Williams and C. Deckard, ‘Advances in modeling the effects of selected parameters on the SLS process’, 1998, *Rapid Prototyping Journal*, Vol. 4, No.2, pp. 90-100.
- [3] S. Kolossov, E. Boillat, R. Glardon, P. Fischer, M. Locher, 2003, ‘3D FE simulation for temperature evolution in the selective laser sintering process’, *International Journal of Machine Tools & Manufacture*, Vol. 44, pp. 117-123.

---

[4] S. Kumpaty, D. Bottrill, A. Hollett, J. Barrett and S. Kamara, 2006, 'An experiment study of heat transfer in selective laser sintering™ process', *9<sup>th</sup> International Conference on Engineering Education*, M5K5-9.

[5] A. Franco, M. Lanzetta, L. Romoli, 2010, 'Experimental analysis of selective laser sintering of polyamide powders: an energy perspective', *Journal of Cleaner Production*, Vol. 18, pp. 1722-1730.

[6] Optics, I, 2010, *BBAR- ZNSE-8-12 Data Sheet*, [http:// www.Isoptics.com](http://www.Isoptics.com).

[7] INSTRON 3340 Series Overview, available at: <http://www.instron.us/wa/product/3300-Single-Column-Testing-Systems.aspx>.